Journal of Ceramic Processing Research. Vol. 18, No. 3, pp. 261~264 (2017)

J O U R N A L O F
Ceramic Processing Research

Graphene supported platinum for oxygen reduction reaction electrocatalyst through a facile microwave-assisted polyol synthesis

Tae-Hyun Kim[a], Jung Hun Yoo[a] and Sung-Chul Yi[a,b,*]

[a]*Department of Chemical Engineering, Hanyang University, Seoul 133-791, Korea*
[b]*Department of Hydrogen and Fuel Cell Technology, Hanyang University, Seoul 133-791, Korea*

In this paper, reduced graphene oxide supported platinum (Pt/rGO) was prepared through a facile microwave-assisted polyol synthesis method. The effect of pH value in the solution during the synthesis on the physicochemical and electrochemical characteristics of the Pt/rGO was investigated. The pH value significantly affected the morphology and chemical state of the Pt nanoparticle due to different hydrolytic components of $PtCl_6^{2-}$ ions. As a result, the highest activity toward the oxygen reduction reaction (ORR) was obtained as 1.372 mA cm^{-2} at 0.9 V from the Pt/rGO prepared from pH 12 which presented 2.63 and 2.09 times higher than the Pt/rGOs prepared at pH 10 and 8, respectively. It is clearly demonstrated that the pH value in the solution is critical for the electrocatalytic performance toward the ORR.

Key words: Proton exchange membrane fuel cell; Oxygen reduction reaction; Graphene supported platinum; Microwave-assisted polyol synthesis.

Introduction

The proton exchange membrane fuel cells (PEMFCs) are one of highly efficient electrochemical energy conversion technologies, with the potential to replace the conventional fossil-fueled power generators for the vehicle and stationary applications. In the conventional PEMFC system, carbon black supported platinum (Pt/C) represents a state-of-the-art electrocatalyst for oxygen reduction reaction (ORR). However, the Pt/C catalysts exhibit severe degradation under the PEMFC operation because of the carbon corrosion [1,2]. Several researchers argued that the degree of graphitization of carbon material is important to alleviate the carbon degradation [3, 4]. Hence, implement of the suitable support materials is necessary to enhance the activity and stability for the ORR catalyst.

Graphene presents a two-dimensional sheet structure composed of the sp^2-bonded carbon atoms with few layers [5, 6]. Graphene has been widely used for various applications such as, methanol oxidation [7], oxygen reduction reaction (ORR) [8,9], hydrogen storage [10], etc., owing to its superior electric conductivity, excellent mechanical stability, and high specific surface area [11-13]. To prepare graphene-based electrocatalysts, previous researchers employed graphene oxide (GO) sheets because of their abundant oxygen functional groups, which exhibit well-dispersed behavior in the aqueous solution. It has been reported that the reduced graphene oxide supported Pt (Pt/rGO) presented higher ORR activity and durability compared to that of the commercial Pt/C [14, 15]. However, there are limitations such as restacking of graphene or agglomeration of the metal nanoparticles due to their high surface energy, hence resulting in decrease in the electrocatalytic activity [16, 17]. Therefore, synthesis of ultrafine Pt nanoparticles deposited on the graphene should be establish to obtain high performance and stable electrocatalysts for the ORR.

In this paper, the Pt/rGO electrocatalysts were synthesized through a facile one-pot microwave-assisted polyol synthesis method without any surfactant. Ethylene glycol (EG) was implemented to simultaneously disperse and reduce the GO and Pt precursor. We report the effect of pH value in the solution on the Pt nanoparticle morphology and electrochemical performances of the Pt/rGO. For the optimized pH value condition, the Pt/rGO presented uniformly dispersed morphology of the Pt nanoparticles and highest ORR activity. In addition, the Pt/rGO presented more durable electrocatalyst compared to the commercial Pt/C.

Experimental

Synthesis of the graphene oxide and catalysts

GO was synthesized by a Tour's method from graphite powder (99.9995%, 200 mesh, Alfa Aesar) [18]. Briefly, the 3 g of graphite powder and 18 g of $KMnO_4$ were mixed in a beaker and added into a 400 ml of mixture of concentrated H_2SO_4/H_3PO_4 (9 : 1 ratio by volume). The mixture was stirred with a heating at 50 °C for 12 h. To quench the reaction, 400 ml of iced

*Corresponding author:
Tel : +82-2-2220-0481
Fax: +82-2-2298-5147
E-mail: scyi@hanyang.ac.kr

DI water and 30% hydrogen peroxide were added into the mixture. After that, the final mixture was centrifuged and washed thoroughly with water, ethanol and 30% HCl.

The Pt/rGO was prepared by the microwave-assisted polyol method. 50 mg of the GO was dispersed into 50 ml of ethylene glycol (EG) (99.5%, Samchun) with stirring 30 min followed by sonication for 1 hr. After that, the H_2PtCl_6/EG solution (1 : 19 ratio by weight) was added drop by drop into the solution with constant agitation and further sonication for 1 hr. The pH value of solution was adjusted for 1 hr by the drop-wise addition of 0.5 M KOH aqueous solution. The Pt/rGOs prepared from pH 8, 10, and 12 are denoted as Pt/rGO1, Pt/rGO2, and Pt/rGO3, respectively. The solution was subjected to the microwave heating for 5 min and cooled to room temperature for 2 hr. Finally, the as-synthesized product was collected by filtration with copious amount of distilled water and ethanol for several times and dried in convection oven at 60 °C for overnight for further characterizations.

Physical characterizations

X-ray diffraction (XRD) patterns of the catalysts were obtained by diffractometer (PW 3040/00 X'PERT, Philips) using Cu Kα X-ray source operating at 40 kV and 30 mA with a scan rate of 2 ° min^{-1} with an angular resolution of 0.05 ° of the 2 theta scan. The morphology of Pt/rGO was obtained by a transmission electron microscopy (TEM) (JEM 2100F, Jeol). In order to evaluate the chemical states of the Pt/rGOs, x-ray photoelectron spectroscopy (XPS) (Theta probe base system, Thermo Fisher Scientific Co.) analysis was implemented with a Al kα X-ray source. The XPS spectra were firstly subtracted the background by Shirley's method and fitted by the Gaussian–Lorentzian method.

Electrochemical characterizations

The electrochemical properties were obtained from a three-electrode electrochemical cell using a rotating disk electrode (RDE) (AFMSRCE, Pine Instrumentation) with a potentiostat/galvanostat workstation (Reference 3000, Gamry). A 0.196 cm^2 area glassy carbon (GC) electrode was employed for the working electrode. A platinum (Pt) wire and Ag/AgCl electrode were used as the counter and reference electrode, respectively. The catalyst ink was prepared dispersing 10 mg of the catalysts and 10 μl of 5 wt% Nafion dispersion (DE521, Ion Power) in 5 ml of ethanol. After homogenization, a predetermined amount of catalyst ink was dropped on the GC electrode and thereby with the Pt loading of 20 μg cm^{-2}. Before characterizing the electrochemical properties, the 0.1 M $HClO_4$ electrolyte was purged with the N_2 gas over 30 min and maintained at 30 °C in a water bath. After then, the catalyst-coated GC was immersed in the electrolyte and electrochemically cleaned through the potential cycling for 50 cycles at 100 mV s^{-1} between 0 and 1.2 V versus reference hydrogen electrode. The ORR activity was evaluated by the LSV at 1600 rpm under the positive scan direction with the scan rate 20 mV s^{-1}. To eliminate the capacitive current contributions, the LSV was conducted under same conditions except for the N_2-saturated electrolyte. The obtained background currents were subtracted from the LSV profiles in the O_2-saturated electrolyte. To examine the effect of support material on the durability of catalyst, an accelerated durability test (ADT) was implemented for the prepared Pt/rGO and the commercial Pt/C. The ADT was performed through the cycling the voltage from 0.6 to 1.0 V with a scan rate of 100 mV s^{-1} under the N_2-saturated condition. During the ADT procedure, the electrochemical surface area (ECSA) was measured for every 200 cycles by cyclic voltammetry in the N_2-saturated electrolyte with the scan rate 50 mV s^{-1}.

Results and Discussion

Physicochemical characterizations

Fig. 1(a) presents the XRD patterns of the Pt/rGOs prepared with different pH values. It is seen that the prepared Pt/rGOs present the diffraction peaks demonstrating Pt(111), Pt(200), Pt(220), and Pt(311), which are consistent to the face-centered cubic structure of Pt (No. JCPDS 65-2868). Figs. 1(b-d) show the TEM images of the Pt/rGOs. After the synthesis procedure, the GO presented a wrinkled structure due to the reduction reaction during Pt deposition. The TEM images exhibit well-deposited Pt nanoparticles on the GOs by the microwave-assisted polyol method. The aggregated morphology of the Pt nanoparticles were obtained from the Pt/rGO1 and Pt/rGO2. On the other hand, the Pt/rGO3 presented

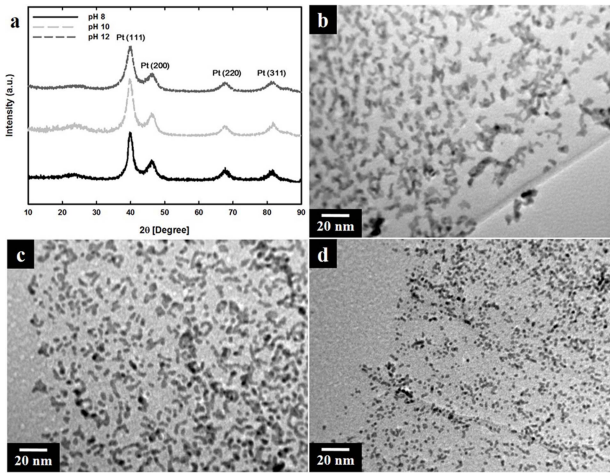

Fig. 1. XRD patterns (a) and TEM images (b-d) of the Pt/rGOs prepared with different pH values. b: Pt/rGO1, c: Pt/rGO2, and d: Pt/rGO3.

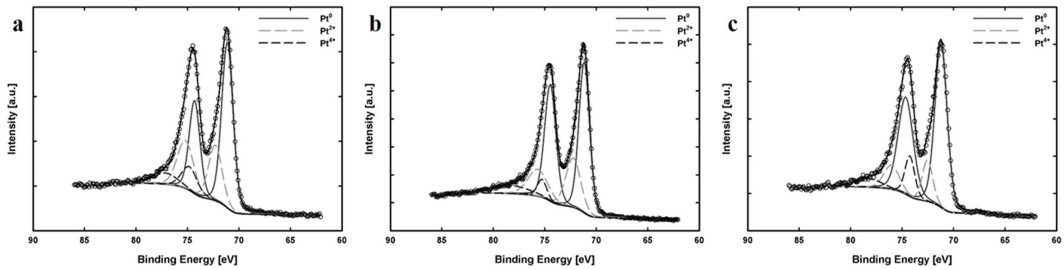

Fig. 2. Pt 4f XPS analysis of the Pt/rGO1 (a), Pt/rGO2 (b), and Pt/rGO3 (c).

Table 1. Summary of the Pt 4f binding energy and relative atomic ratio among the species.

	Binding energy of peak [eV]		Relative atomic ratio [at.%]		
Sample	Pt $4f_{5/2}$	Pt $4f_{7/2}$	Pt^0	Pt^{2+}	Pt^{4+}
Pt/rGO1	74.48	71.25	57.02	30.32	12.65
Pt/rGO2	74.54	71.25	63.17	27.36	9.48
Pt/rGO3	74.58	71.28	71.15	16.61	12.24

uniformly-distributed Pt nanoparticles with 2-3 nm particle sizes, indicating that the pH value significantly affects the distribution of Pt nanoparticles. The pH value affects the hydrolytic components of $PtCl_6^{2-}$ ions during the Pt deposition process [19]. As increasing the pH value in the solution, the hydrolysis of $PtCl_6^{2-}$ ions lead to $Pt(OH)_xCl_{6-x}^{2-}$ with fewer chlorides, thereby resulting in uniformly deposited Pt morphology on the GO. Therefore, high value of pH in the solution is beneficial to obtain the Pt nanoparticles with uniformly distributed morphology.

XPS analysis was implemented to examine the chemical state of Pt species of the Pt/rGOs prepared from different pH values. Fig. 2 and Table 1 present the Pt 4f XPS spectra and summary of the results of fits of spectra, respectively. Generally, the Pt/rGOs exhibited three sets of doublets at approximately 71.4 and 74.8 eV, 72.4 and 75.8 eV, and 75.2 and 78.6 eV indicating the metallic Pt, Pt(II), and Pt(IV), respectively. For the Pt/rGO3, it presented most positive shift of the Pt $4_{f5/2}$ and Pt $4f_{7/2}$ peaks compared to the other catalysts, indicating enhanced interaction between the Pt and the support material. In addition, the Pt/rGO3 showed highest ratio of the metallic Pt compared to the other Pt/rGOs. It can be concluded that the morphology of the deposited Pt affects the chemical state of the Pt species.

Electrochemical characterizations

Fig. 3 presents the electrochemical characterizations of the prepared catalysts. Fig. 3(a) shows the ORR activities of the Pt/rGOs prepared from different pH values. As observed in Fig. 3(a), the Pt/rGO3 exhibited highest ORR activity among the prepared Pt/rGOs. Specifically, the Pt/rGO3 presented 1.372 mA cm^{-2} at 0.9 V, while the Pt/rGO1 and Pt/rGO2 showed 0.521 and 0.657 mA cm^{-2}, respectively. It can be concluded

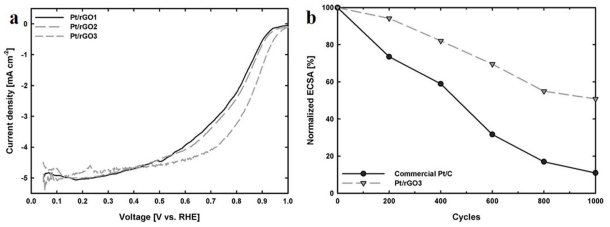

Fig. 3. ORR activities of the prepared Pt/rGOs (a) and normalized ECSA values of the Pt/rGO3 and commercial Pt/C throughout the ADT.

that the mono-dispersed Pt morphology improves the catalytic activity toward the ORR. In addition, the positive shift of peaks and high atomic ratio of the Pt metallic in the Pt/rGO3 improved the ORR activity. Hence, the pH value in the microwave-assisted polyol method is critical in preparing high electrocatalytic activity toward the ORR. In order to investigate the durability of the Pt/rGO, the ADT procedure was employed for the Pt/rGO3 and commercial Pt/C. The ECSA values of the Pt/rGO3 and commercial Pt/C were evaluated for every 200 cycles during the ADT and exhibited in Fig. 3(b) as normalized ECSA values. As observed in Fig. 3(b), the ECSA of the Pt/rGO3 retained 51% of the initial ECSA of the Pt/rGO3, whereas the commercial Pt/C maintained 21% of the initial ECSA. The enhanced durability of the Pt/rGO3 is attributed to the relatively higher graphitic content of graphene than amorphous carbon black and improved bonding strength between the Pt and support material.

Conclusions

In summary, this paper reports the effect of the pH value in the solution on the physicochemical and electrochemical properties of the Pt/rGOs. From the TEM images, the pH values significantly affect the morphology of deposited Pt nanoparticles on the graphene due to different hydrolytic components of $PtCl_6^{2-}$ ions. The Pt/rGO prepared at pH 12 presented mono-dispersed morphology of the Pt nanoparticles on the graphene, while the Pt/rGOs synthesized at pH lower than 10 exhibited aggregated Pt nanoparticles. The Pt 4f XPS spectra of the Pt/rGO3 presented positive shift of peak with higher atomic ratio of metallic Pt compared to the other catalysts. It is clearly

demonstrated that the ORR activity was improved by increasing the pH value in the solution due to uniformly dispersed Pt morphology with high metallic Pt content. In addition, the Pt/rGO3 showed the improved durability owing to the high graphitic content and enhanced bonding strength between the Pt and carbon support compared to the commercial Pt/C. The present work highlights the importance of the pH value in the synthesis process to achieve high activity and durable electrocatalysts toward the ORR.

Acknowledgments

This research was supported by the Commercializations Promotion Agency (2016K000147) for R & D Outcomes (COMPA) funded by the Ministry of Science, ICT and Future Planning (MSIP).

References

1. J. Wu, X. Z. Yuan, J. J. Martin, H. Wang, J. Zhang, J. Shen, S. Wu, and W. Merida.
2. J. Power Sources 184 (2008) 104-119.
3. Y.J. Wang, D.P. Wilkinson, and J. Zhang. Chem. Rev. 111 (2011) 7625-7651.
4. D. Bom, R. Andrews, D. Jacques, J. Anthony, B. Chen, M.S. Meier, and J.P. Selegue. Nano Lett. 2 (2002) 615-619.
5. M. Kang, Y.S. Bae, and C.H. Lee. Carbon 43 (2005) 1512-1516.
6. S. Stankovich, D.A. Dikin, G.H.B. Dommett, K.M. Kohlhaas, E.J. Zimney, E.A. Stach, R.D. Piner, S.T. Nguyen, and R.S. Ruoff. Nature 442 (2006) 282-286.
7. Y. Zhu, D.K. James, and J.M. Tour. Adv. Mater. 24 (2012) 4924-4955.
8. Y.M. Li, L.H. Tang, and J.H. Li. Electrochem. Commun. 11 (2009) 846-849.
9. T. Maiyalagan, X. Dong, P. Chen, and X. Wang. J. Mater. Chem. A 22 (2012) 5286-5290.
10. D. He, K. Cheng, H. Li, T. Peng, F. Xu, S. Mu, and M. Pan. Langmuir 28 (2012) 3979-3986.
11. R. Strobel, J. Garche, P.T. Moseley, L. Jorissen, and G. Wolf. J. Power Sources 159 (2006) 781-801.
12. K.S. Novoselov, A.K. Geim, S.V. Morozov, D. Jiang, M.I. Katsnelson, I.V. Grigorieva, S.V. Dubonos, and A.A. Firsov. Nature 438 (2005) 197-200.
13. Y.B. Zhang, Y.W. Tan, H.L. Stormer, and P. Kim. Nature 438 (2005) 201-204.
14. H. Yang, Q. Zhang, C. Shan, F. Li, D. Han, and L. Niu. Langmuir 26 (2010) 6708-6712.
15. D. Higgins, M.A. Hoque, M.Ho. Seo, R. Wang, F. Hassan, J.Y. Choi, M. Pritzker, A. Yu, J. Zhang, and Z. Chen. Adv. Funct. Mater. 24 (2014) 4325-4336.
16. J. Zhu, G. He, Z. Tian, L. Liang, and P.K. Shen. Electrochim. Acta 194 (2016) 276-282.
17. P.V. Kamat. J. Phys. Chem. Lett. 1 (2009) 520-527.
18. L. Shang, T. Bian, B. Zhang, D. Zhang, L.Z. Wu, C.H. Tung, Y. Yin, and T. Zhang. Angew. Chem. Int. Edit. 53 (2014) 250-254.
19. D.C. Marcano, D.V. Kosynkin, J.M. Berlin, A. Sinitskii, Z. Sun, A. Slesarev, L.B. Alemany, W. Lu, and J.M. Tour. ACS Nano 4 (2010) 4806-4814.
20. F. Zhang, J. Chen, X. Zhang, W. Gao, R. Jin, N. Guan, and Y. Li. Langmuir 20 (2004) 9329-9334.